

# Slaking mechanisms of mudstone liner immersed in water

Tzong-Tzeng Lin <sup>a,\*</sup>, Chyi Sheu <sup>a</sup>, Juu-En Chang <sup>b</sup>,  
Chih-Hung Cheng <sup>b</sup>

<sup>a</sup> Department of Civil Engineering, National Kaohsiung Institute of Technology, 415 Chien-Kung Rd.,  
Kaohsiung 80782, Taiwan

<sup>b</sup> Department of Environmental Engineering, National Cheng Kung University, Tainan, Taiwan

---

## Abstract

The purpose of this research is to probe the slaking property of the mudstone meeting with water. The elemental, crystalline, and morphologic changes in the mudstone with three different water contents were characterized using X-ray fluorescence spectrometer (XRF), semi-dynamic leach test, X-ray diffractometer (XRD), and scanning electron microscopy (SEM)/energy-dispersive X-ray analysis (EDAX) techniques. The XRF and chemical composition analyses indicated that the mudstone contains high concentrations of silicon and aluminum and low concentrations of calcium, iron, potassium, and sodium. The XRD examination showed large amount of quartz and illite, minor calcium aluminate hydrate and calcium silicate hydrate, and small amount of unidentifiable peaks. The result of semi-dynamic leach test showed that the release of sodium is very rapid initially and the released calcium species increase largely in the final subsequent extractions. The microanalysis using SEM/EDAX indicated that the petal-like structures increase with the moisture content of the mudstone. Thus, it was inferred that the possible mechanisms of the mudstone meeting with water to lead to the slaking phenomenon are stated as follows. The sodium sulfate will rapidly dissolve from the mudstone, and the sulfate species and calcium aluminate hydrate form the platelet-like solid solution of  $3\text{CaO}-\text{Al}_2\text{O}_3-\text{CaSO}_4 \cdot 12\text{H}_2\text{O}$  making the mudstone lose its cementing reaction. © 1998 Elsevier Science B.V.

*Keywords:* Slaking; Mudstone; Scanning electron microscopy

---

## 1. Introduction

More recently, the high-density polyethylene (HDPE) geomembrane has widely been used as the circumference and bottom liners to preventing for leachate seepage at

---

\* Corresponding author.

Taiwan's sanitary landfill. The minimum thickness specification for a synthetic flexible membrane liner is 2.0 mm. Such landfill can be turned into a contaminated zone due to its bad construction quality or improper operation. For compacted, low permeability bottom liners, the US Environmental Protection Agency guidance recommends clay materials, and the compacted clay bottom liner must be sufficiently thick to prevent hazardous constituent migration [1,2].

Although many researchers have been devoted to study the issues related to landfill liners, especially clay materials, it is difficult to obtain large amount of clay materials in Taiwan [3,4]. Conversely, the mudstone is widely and deeply distributed over the southwestern Taiwan. Considering the results of research reports [5,6] concerned to mudstone from the standpoint of civil engineering for provision against natural disasters, the physical properties of mudstone seem to meet the soil properties of landfill liner recommended by Benson et al. [7].

The mudstone belongs to marine deposit. Due to its complex composition and typical property, there is poor understanding of the feasibility of mudstone material applied on landfill soil liner. Thus, the aim of this study is to explore the slaking property of the mudstone meeting with water. The elemental, crystalline, and morphologic changes in the mudstone with three different water contents were characterized by using X-ray fluorescence spectrometer (XRF), semi-dynamic leach test, X-ray diffractometer (XRD), and scanning electron microscopy (SEM)/energy-dispersive X-ray analysis (EDAX) techniques. The understanding of such phenomenon would be useful to explain the hydraulic conductive behavior of water across the mudstone liner. It is further expected that the mudstone material could be designed for replacing the clay material as a natural landfill liner.

## 2. Materials and methods

### 2.1. Material

The raw mudstone was used as a natural liner material in this work. Raw mudstone was directly drilled from Nei-men area, Kaohsiung county, Taiwan. A series of semi-dynamic leaching tests on the mudstone was performed using purity water produced by reverse osmosis to simulate the continuous rainfall situations. The mudstone sample was likely to contain soil material and required pretreatment before total metal analysis. Pretreatment included alkalis ( $\text{Li}_2\text{B}_4\text{O}_7$ ) and acid (1 + 1 redistilled HCl) addition to decompose the mudstone and bring all metals into solution. All the chemicals used in this work were reagent-grade products.

### 2.2. Sample preparation

The chemical composition sample was prepared first by mixing 0.8 g  $\text{Li}_2\text{B}_4\text{O}_7$  and 0.1 g mudstone. The mixture was coated with a layer of  $\text{Li}_2\text{B}_4\text{O}_7$ , heated at  $1100^\circ\text{C}$  for 1 h, followed by air quenching, and then 150 ml 1 + 1 redistilled HCl were added to melt all metals into solution [8]. The dried mudstone was manually crushed to pass

#100 sieve before XRD and XRF examinations. The samples for SEM/EDAX were prepared first by mixing each 5 g mudstone with pure water to make the mudstone with 25%, 45%, and 65% moisture contents, respectively. A set of three samples was dried by using vacuum freeze drier. A few dried samples were then put on a copper specimen holder and coated with thin carbon film for SEM observations.

### 2.3. Analysis

Elemental qualitative analysis of mudstone was performed by using Rigaku XRF (Model 3063M). Operation parameters were 40 kV and 10 mA. The solution for total metal's analysis was obtained by using Jobin Yvon Inductively Coupled Plasma (ICP, Model JY 38 Plus). Pulverized and sieved sample was used for XRD analysis with a Max III X-ray diffractometer. Operation parameters for CuK  $\alpha$  radiations were 30 kV and 20 mA. The measured intensities and  $2\theta$  values were recorded and analyzed by a computer system. The samples were scanned from  $5^\circ$  to  $80^\circ$ . Semi-dynamic leaching is a process in which the leachant is renewed periodically after intervals of static leaching. A water/mudstone weight ratio of 10:1 was used in the leaching tests and the leachant in contact with mudstone was replaced with new pure water on a 24 h basis. The combined decanted solution was filtered through  $0.45 \mu\text{m}$  membrane paper and the filtrate was used for total elemental analysis using ICP. A set of three samples was coated with carbon thin film for morphology observations using SEM and micro-probe and area analyses by EDAX (Hitachi SEM S-2500 with a Link LZ-5 EDAX). The SEM was operated at 20 keV accelerating voltage under a vacuum chamber pressure of less than  $5 \times 10^{-5}$  Torr.

## 3. Results and discussion

### 3.1. Qualitative / quantitative analyses using XRF and ICP

Fig. 1 illustrates a qualitative analysis of the X-ray fluorescence method for raw mudstone. Identification of peaks is then accomplished by reference to tables of emission lines of the elements. The results clearly show that the mudstone contains high concentrations of silicon, aluminum, calcium, iron, and potassium, and low concentrations of sodium, sulfur, magnesium, chlorine, titanium, and strontium. The qualitative information shown in Fig. 1 can supply a choice of elements for quantitative analysis using ICP.

The quantitative information from ICP analysis for chemical composition of raw mudstone is presented in Table 1. It indicates that the major elements of raw mudstone are in the order of  $\text{Si} > \text{Al} > \text{Ca} > \text{Fe} > \text{K} > \text{Na} > \text{Mg}$ . Moreover, it certainly affords a sound basis for crystalline identification of raw mudstone determined by XRD.

### 3.2. X-ray diffraction

XRD is an excellent tool to study the changes in crystallinity and appearance or disappearance of phases [9]. The file shown in Joint Committee on Powder Diffraction

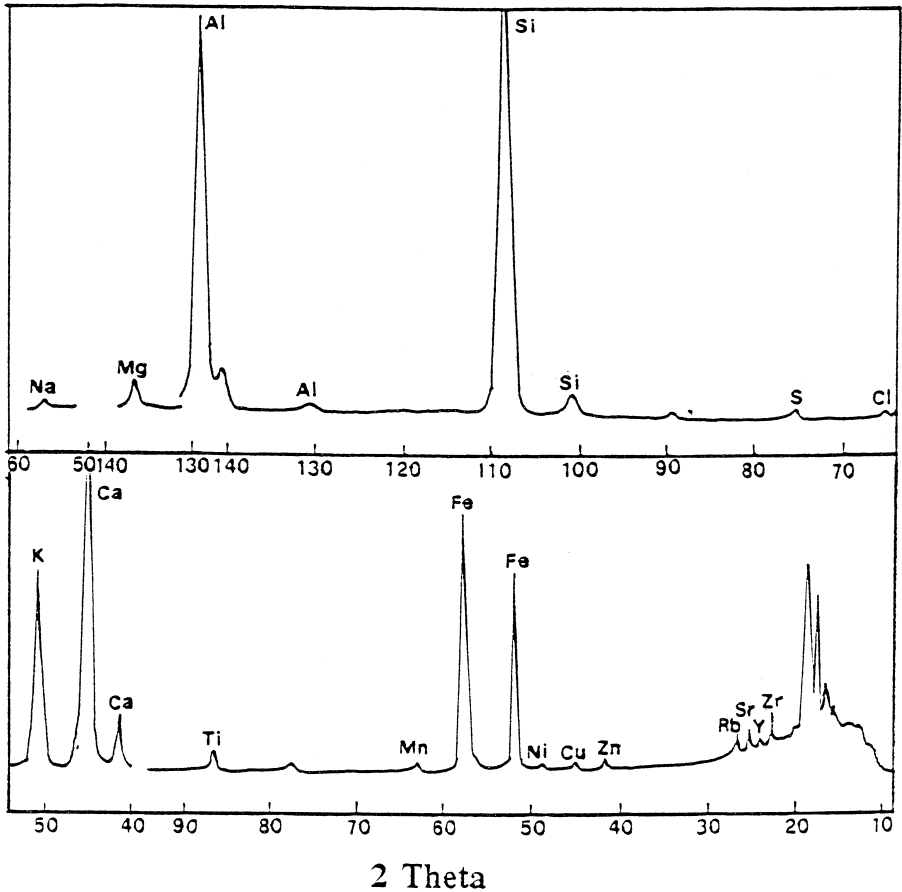


Fig. 1. X-ray fluorescence spectrum for fresh mudstone recorded with a wavelength spectrometer.

Standards (JCPDS) is used to identify various crystalline phases. The qualitative XRD pattern for raw mudstone is shown in Fig. 2. The result obviously reveals large amount of quartz (JCPDS pattern number: 33-1161) and illite (JCPDS pattern number: 26-911), minor calcium aluminate hydrate (JCPDS pattern number: 12-408 for  $\text{CaO}-\text{Al}_2\text{O}_3 \cdot 10\text{H}_2\text{O}$ , abbreviated as  $\text{CAH}_{10}$ ) and calcium silicate hydrate (JCPDS pattern number: 33-306 for  $1.5\text{CaO}-\text{SiO}_2 \cdot x\text{H}_2\text{O}$ , abbreviated as CSH), and small amount of unidentifiable peaks.

Yao [10] studied the physical, chemical, and mechanical properties of raw mudstone. He found that raw mudstone can be categorized as sand, silt, and clay according to texture fractions and can be in possession of high uniaxial compressive strength before immersed in water. Considering the above results, it is intended to infer that the major crystalline phase of sand is quartz, the main phase of clay is illite, and silt principally contains silica, alumina, and calcium oxide. Since silicon, aluminum, and calcium oxides have pozzolanic characteristics, the cementing reaction has brought about their

Table 1  
Chemical composition of raw mudstone

Constituent	% By weight
SiO <sub>2</sub>	48.27
Al <sub>2</sub> O <sub>3</sub>	17.23
CaO	6.04
Fe <sub>2</sub> O <sub>3</sub>	5.90
K <sub>2</sub> O	4.67
Na <sub>2</sub> O	4.25
MgO	2.72
CuO	0.39
SrO	0.09
MnO	0.06
ZnO	0.05
NiO	0.02

gelatinous hydrates in a normal environment [11]. Thus, the crystalline analysis of raw mudstone does exist CAH<sub>10</sub> and CSH. The raw mudstone possesses more compressive strength that is probably attributed to the cementation between clay and sand formed by pozzolanic hydrates.

### 3.3. Semi-dynamic leach test

The purpose for conducting the semi-dynamic leach test was to determine the release of which species is dissolution-controlled in the liquid phase of mudstone immersed in water. The cumulative release of various elements from the raw mudstone under the

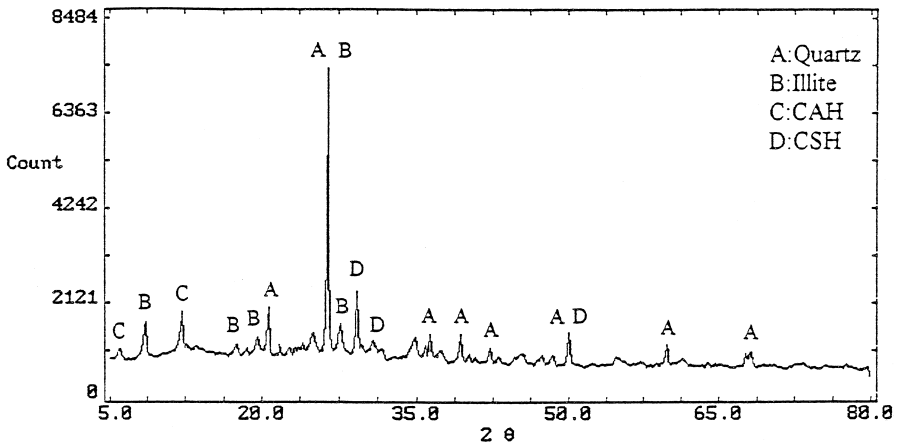


Fig. 2. XRD patterns of fresh mudstone. Symbols are as follows: (A) SiO<sub>2</sub>; (B) (K, H<sub>3</sub>O)[Al<sub>2-x</sub>(Mg-Fe)<sub>x</sub>](Si<sub>4-x</sub>Al<sub>x</sub>)O<sub>10</sub>(OH)<sub>2</sub>; (C) calcium aluminate hydrate (CaO–Al<sub>2</sub>O<sub>3</sub>·10H<sub>2</sub>O); (D) calcium silicate hydrate (1.5CaO–SiO<sub>2</sub>·xH<sub>2</sub>O).

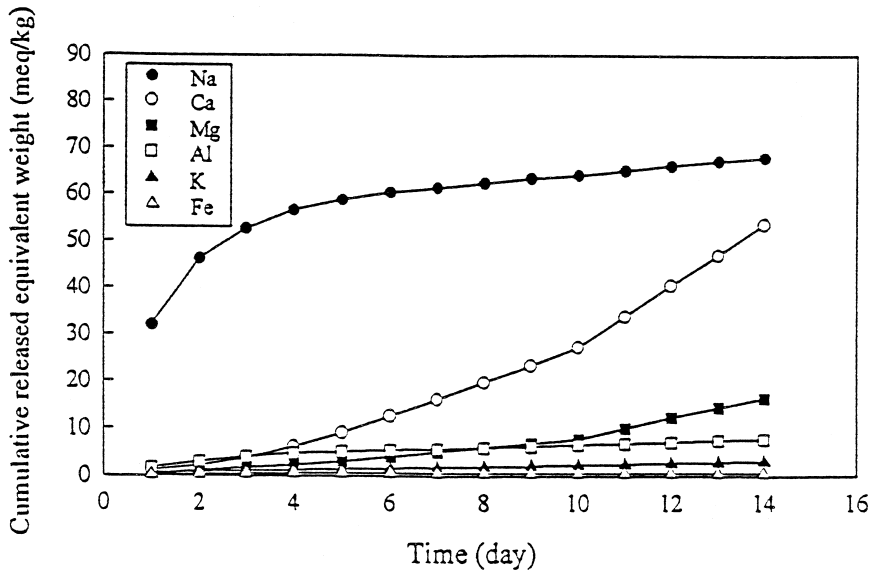


Fig. 3. Cumulative equivalent weight of Na, Ca, Mg, Al, K, and Fe leached out of the fresh mudstone using semi-dynamic leaching procedures.

dissolution of pure water is shown in Fig. 3. This result was generated by measuring the leachate concentrations after each leaching period and calculating the cumulative equivalent weight leached for each element. Comparing the different cumulative curves, it can be found that the degree of dissolution of various elements from the solid phase can be classified as:  $\text{Na}^+ > \text{Ca}^{2+} > \text{Mg}^{2+} > \text{Al}^{3+} > \text{K}^+ > \text{Fe}^{3+}$ . Clearly, the release of Na is very rapid; in about five extractions, the amount of Na released reached the maximum, 60 meq/kg in the system. The release of Ca increased constantly in a 14 day period of extraction, corresponding to 50 meq/kg. On the contrary, the leaching of Mg, Al, K, and Fe was insignificant; 5 meq/kg at most for magnesium ion was transferred to the solution even after 10 extractions.

The results of the cumulative equivalent weight of various metals leached out of the raw mudstone obviously reveal that the degree of dissolution of magnesium, aluminum, iron, and potassium ions is hardly discernible. It infers that the clay phase of mudstone does not decompose as the mudstone is immersed in water. Moreover, based on the large amount of sodium ion leached out of mudstone in the initial extraction, it probably implies that the sodium species might play a role in slaking the moisten mudstone.

Cheng [12] investigated the low-lying land of the fresh mudstone region drenched with rain. He found that the surface of the dried mudstone formed a layer of white crystals. An X-ray diffraction analysis of this crystal showed that it was sodium sulfate.  $\text{Na}_2\text{SO}_4$  is a salt, so it dissociates to produce  $\text{Na}^+$  and  $\text{SO}_4^{2-}$ . According to the literature [13], calcium aluminate hydrate can recrystallize with sulfate species to form the high-sulfate sulfoaluminate ( $3\text{CaO}-\text{Al}_2\text{O}_3-3\text{CaSO}_4 \cdot 32\text{H}_2\text{O}$ , abbreviated as Aft) or the hexagonal-plate solid solution ( $3\text{CaO}-\text{Al}_2\text{O}_3-\text{CaSO}_4 \cdot 12\text{H}_2\text{O}$ , abbreviated as Afm) and

to lead to volume expansion. Thus, based on the above results, it is suggested that the slaking mechanisms of mudstone immersed in water are summarized as follows: (1) sodium sulfate contained in mudstone meet with water to dissociate into  $\text{Na}^+$  and  $\text{SO}_4^{2-}$ ; (2) sulfate species and calcium aluminate hydrate produces the needle-like Aft or the platelet-like Afm phases; (3) the cementation between two major mudstone constituents (sand and clay) destroys due to volume expansion, and then the mudstone gradually decomposes to lead to the slaking phenomenon.

### 3.4. Microanalysis using SEM / EDAX

It is reasonable to assume that if the addition of water alters the physical structure of the mudstone, the ability of the mudstone to agglomerate its textural fractions will also be affected. Therefore, useful information may be obtained by the observation of morphological characteristics of a set of wet mudstone using SEM. Microchemical analysis using the SEM/EDAX technique provided useful information on the understanding of elemental change after raw mudstone absorbed moisture. The microstructure from raw mudstone is shown in Fig. 4a. It clearly shows that many grains are in a flat-like structure and some platelet-like phase is enveloped in the flat grain. The microprobe analysis of the flat grain (A in Fig. 4a) measured high concentrations of silicon, potassium, aluminum, iron, and magnesium and low concentration of calcium. Based on chemical structure of illite,  $(\text{K}, \text{H}_3\text{O})[\text{Al}_{2-x}(\text{Mg} \cdot \text{Fe})_x](\text{Si}_{4-x}\text{Al}_x)\text{O}_{10}(\text{OH})_2$ , the percentage of each major element is of about the same quantity. From this we may infer that high concentration of silicon is partly contributed from sand and silt and low concentration of calcium is possibly supplied from calcium silicate and calcium aluminate hydrates. Thus, it implies those texture fractions (sand, clay, and silt) have compacted and cemented into the flat grain. According to Cheng [12], the platelet-like structure is probably identified as illite phase by SEM/EDAX technique.

SEM micrograph of mudstone containing 25% water content as depicted in Fig. 5a does reveal a few of platelet-like phases on the surface of grain. Through the elemental area analysis by EDAX as shown in Fig. 5b, it can identify that the concentration of silicon, aluminum, potassium, and iron does not obviously differ from the result of Fig. 4b. However, due to an increase in the concentration of calcium, it implies that the calcium species have gradually transferred to the outer surface after raw mudstone absorbed a little water.

Fig. 6a displays the morphology of mudstone bearing 45% moisture content where a large amount of platelet-like structures is present in the micrograph. This demonstrates that the entrapped platelet-like phases in the flat grain are not deeply affected by the cementation. An EDAX spectrum as presented in Fig. 6b reveals a decrease in silicon species and an obvious increase in calcium species. This may infer that the cementation is totally destroyed after mudstone absorbed high moisture to lead to separations of sand and clay.

The microstructure of mudstone containing 65% water content as shown in Fig. 7a clearly shows a serious collapse of the flat grain. The microchemical analysis by EDAX as presented in Fig. 7b reveals an apparent decrease in silicon species and an evident increase in calcium species. The low concentration of silicon on the outer surface of

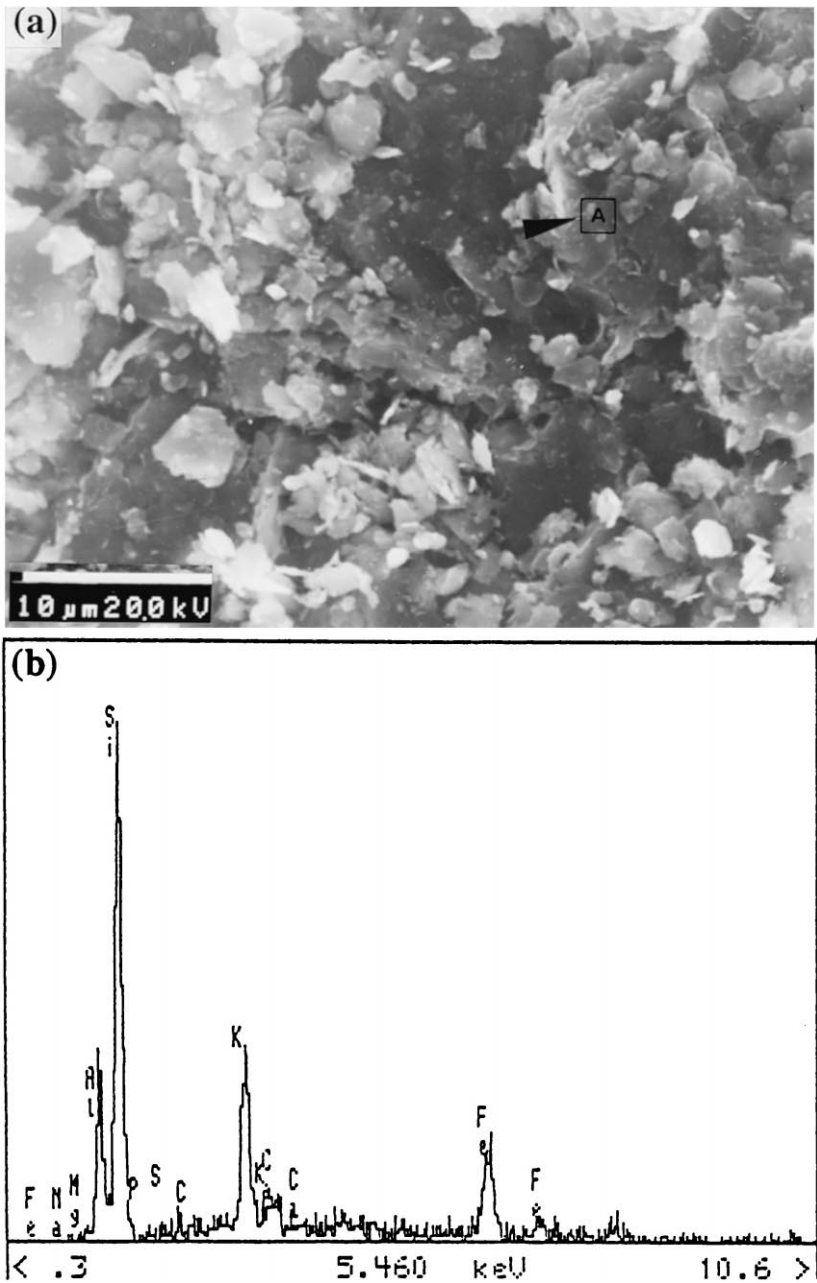


Fig. 4. (a) SEM micrograph of the fresh mudstone showing a lot of rock-like grains; microprobe analysis of the region with (b) the label A.



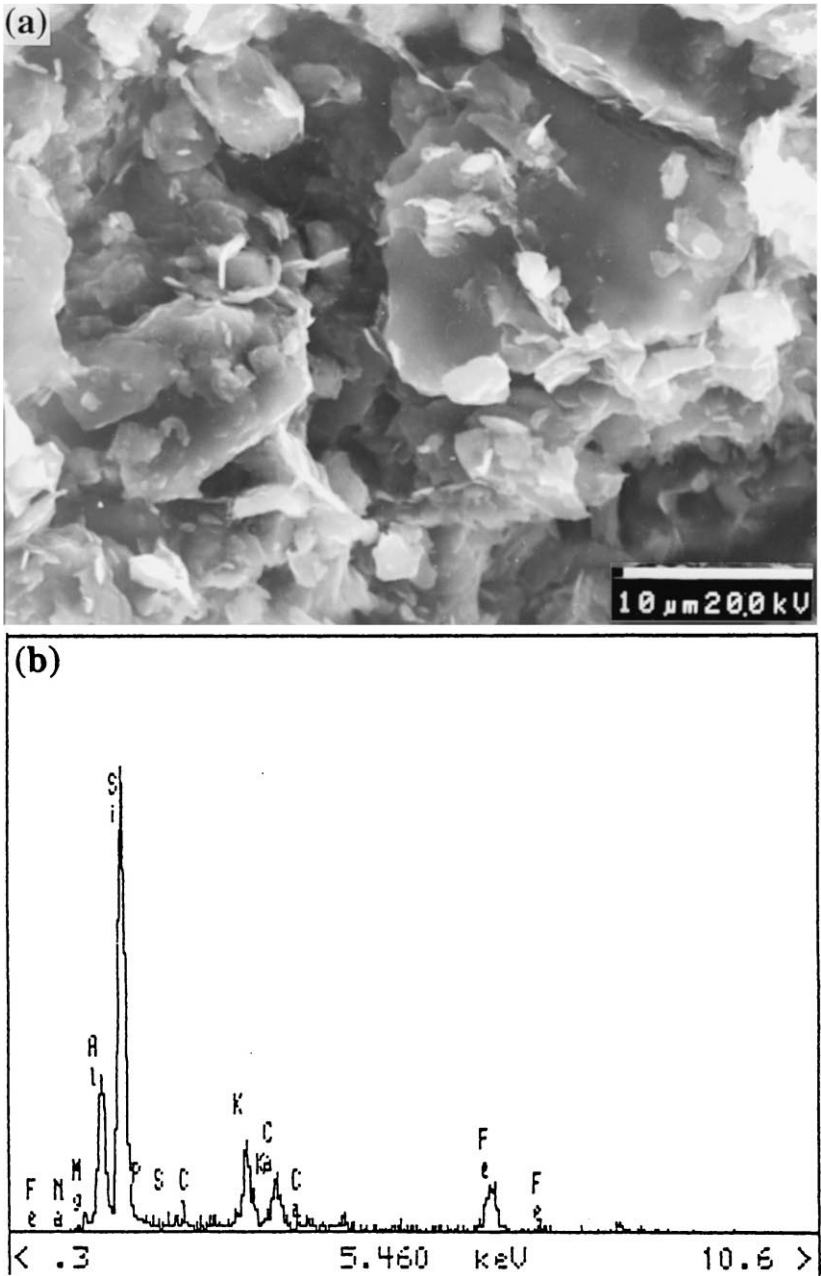


Fig. 5. (a) SEM micrograph of the mudstone with 25% moisture showing the presence of petal-like structure on the surface of grain; (b) area analysis of EDAX in (a) to be lean in Ca.

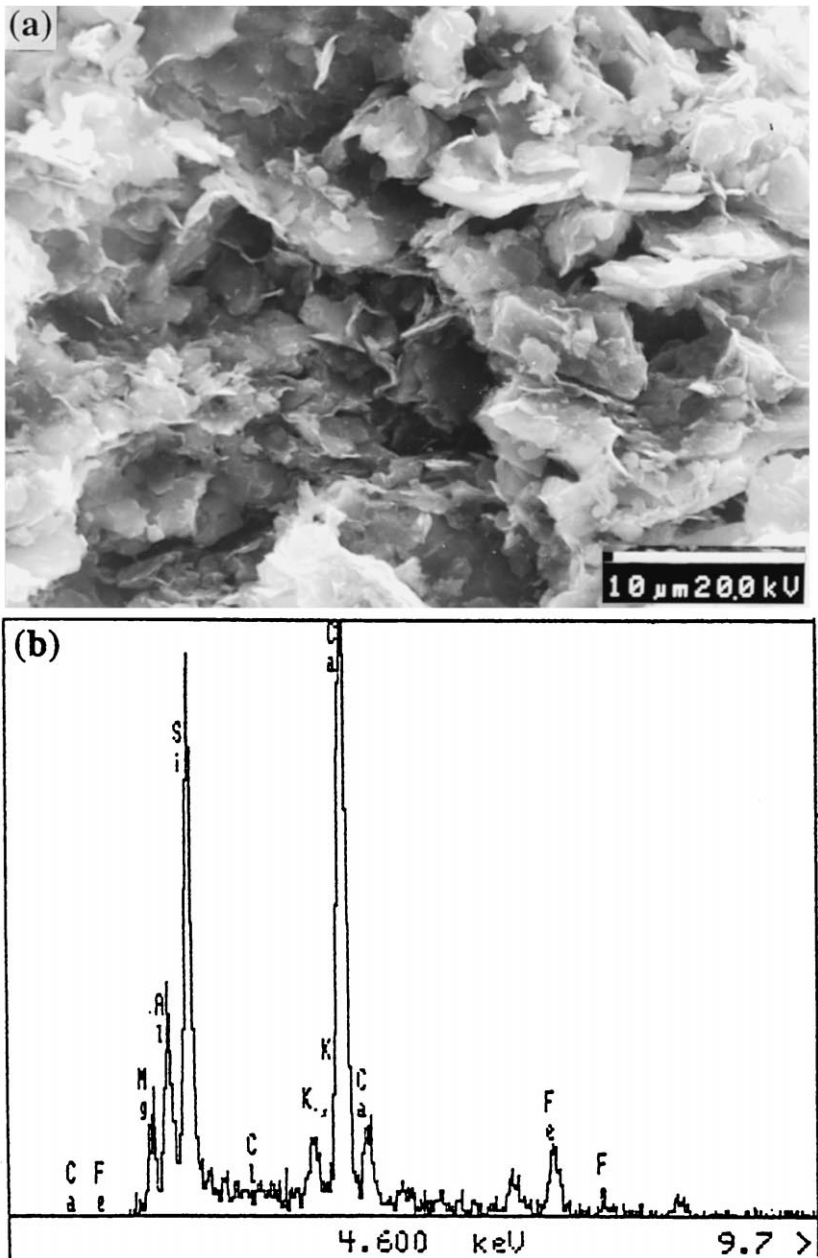


Fig. 6. SEM micrograph of the mudstone with 45% moisture showing plenty of petal-like matter; area analysis of EDAX in (a) to be rich in Ca.

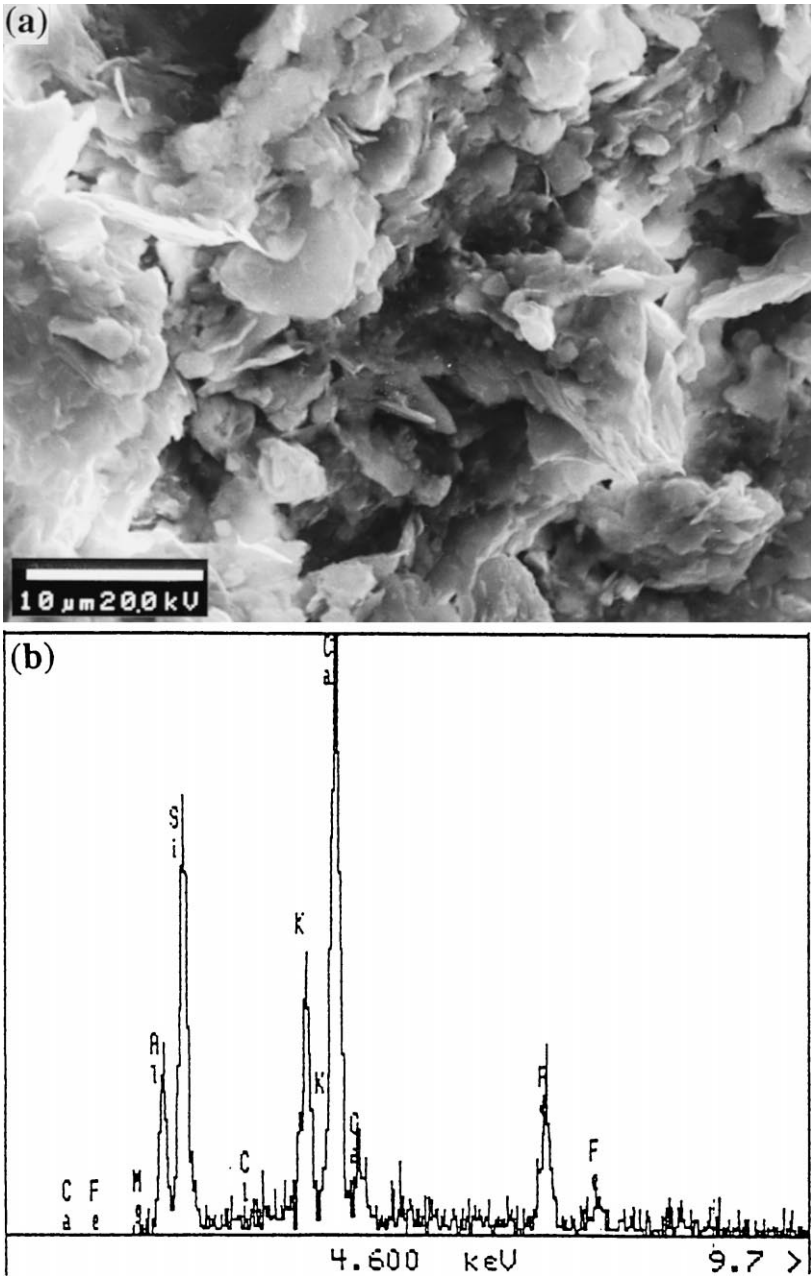


Fig. 7. SEM micrograph of the mudstone with 65% moisture showing a large amount of rosette-like structure; area analysis of EDAX in (a) to be rich in Ca.

mudstone is possibly attributed to the settlement of the isolated sand under a much moist environment.

The results of SEM/EDAX analyses are consistent with the findings of semi-dynamic leach test where the slaking phenomenon is due to the mudstone absorbed moisture. Based on the microanalysis, the destruction of mechanical strength after the mudstone absorbed water is not due to an increase in porosity. The morphological structures of each major textural fraction in the different moisten mudstones can effect no change of importance, but a lot of platelet-like structures distinctly exist in the dampen mudstone. We were, therefore, able to infer that the reaction between sulfate species and calcium aluminate hydrate leads to the formation of platelet-like Afm phase. Consequently, it is probably suggested that little uniaxial compressive strength after mudstone absorbed high moisture is attributed to the decomposition of the products of pozzolanic reaction in the mudstone.

#### 4. Conclusion

The use of XRF, ICP, XRD, and SEM/EDAX techniques and semi-dynamic leach test has provided valuable information regarding the slaking mechanisms of mudstone absorbed moisture. Based on the results of XRF, ICP, XRD, semi-dynamic leach test, and SEM/EDAX, the slaking mechanisms of mudstone immersed in water are summarized as follows: (1) sodium sulfate contained in mudstone meet with water to dissociate into  $\text{Na}^+$  and  $\text{SO}_4^{2-}$ ; (2) sulfate species and calcium aluminate hydrate produces the hexagonal-plate solid solution of Afm phase; (3) little uniaxial compressive strength after mudstone absorbed water is due to the decomposition of cementation in the mudstone and volume expansion in the inner mudstone; (4) then the mudstone gradually decomposes with its moisture content to lead to the slaking phenomenon. The results would be very significant for understanding and explaining the hydraulic conductive behavior of water across the mudstone liner and will be helpful for future work that the mudstone material could be designed for replacing the clay material as a natural landfill liner.

#### Acknowledgements

This study was funded by the National Science Council of R.O.C. under contract No. NSC 85-2211-E151-003.

#### References

- [1] D.E. Danial, Earthen liners for land disposal facilities, Proc. Geotechnical Practice for Waste Disposal, ASCE, 1987, pp. 21–39.
- [2] USEPA, Design, construction, and evaluation of clay liners for waste management facilities, EPA/530/SW-86/007, Cincinnati, OH, 1992.

- [3] C.C. Fan, Influence of organic fluid on hydraulic conductivity of clay, Master Thesis, National Taiwan University, Taipei, Taiwan, R.O.C., 1992.
- [4] C.W. Cheng, Physical transport of bromide through compacted soils, Master Thesis, National Chung Hsing University, Taichung, Taiwan, R.O.C., 1993.
- [5] D.H. Lee, A study on shear strength characteristics of mudstone, National Science Council, NSC 77-0414-P006-13B, Taipei, Taiwan, 1989.
- [6] F.S. Yen, Relationships between morphology and weathering-erosion behavior of mudstone slopes in the Southwestern Taiwan, National Science Council, NSC 75-0414-P006-04, Taipei, Taiwan, 1987.
- [7] C.H. Benson, H. Zhai, Z. Wong, Estimating hydraulic conductivity of compacted clay liners, *J. Geotech. Eng.* 120 (1994) 366–387.
- [8] C.C. Shey, Resource of zeolite converted by fly ash, Master Thesis, National Taiwan University, Taipei, Taiwan, 1994.
- [9] F.K. Cartledge, H.C. Eaton, M.E. Tittlebaum, Morphology and microchemistry of solidified/stabilized hazard, Waste Systems, Risk Reduction Engineering Laboratory, EPA/600/2-89/056, Cincinnati, OH, 1989.
- [10] M.L. Yao, Permeability and diffusion of compacted mudstone, Master Thesis, National Cheng Kung University, Tainan, Taiwan, 1993.
- [11] R.L. Terral, J.A. Epps, E.J. Barenberg, J.K. Mitchell, M.R. Thompson, Soil stabilization in pavement structures, A User's Manual, Vol. 2, Mixture Design Considerations, FHWA, DOT, Washington, 1979.
- [12] C.H. Cheng, Feasibility of use of mudstone material as a natural landfill liner, Master Thesis, National Cheng Kung University, Tainan, Taiwan, 1996.
- [13] F.M. Lea, *The Chemistry of Cement and Concrete*, 3rd edn., Edward Arnold, London, 1970.